

Covariant light front perturbation theory and three-particle equations

Michael G. Fuda

Department of Physics and Astronomy, State University of New York at Buffalo, Buffalo, New York 14260

(Received 24 March 1986)

A covariant version of light front perturbation theory is obtained as a limit of the covariant time-ordered perturbation theory developed recently by the author. The graphical rules for the covariant light front perturbation theory are essentially the same as Weinberg's infinite momentum frame rules; however, they involve a redefinition of the original Weinberg variables. The new definitions guarantee that the contributions of individual diagrams to the S matrix are invariant. A set of manifestly invariant three-particle integral equations is derived. These equations are obtained from a model field theory which describes the interaction of a charged scalar particle ψ with a neutral scalar particle ϕ according to the virtual process $\psi\bar{\psi}\rightarrow\psi+\phi$. The solutions of the integral equations lead to amplitudes for $\phi+\psi\rightarrow\phi+\psi$ and $\phi+\psi\rightarrow2\phi+\psi$ which satisfy two- and three-particle unitarity. The integral equations are free of the spurious singularity in s , the square of the invariant c.m. energy, which has been an undesirable feature of earlier relativistic three-particle equations. This singularity is known to be responsible for spurious bound state solutions.

I. INTRODUCTION

Quantum field theories are commonly analyzed by developing perturbation series for the S matrix. In the most popular version of perturbation theory, the various terms of the series are represented by Feynman diagrams.¹ In these diagrams the total four-momentum is conserved at each vertex, the intermediate particles are off-the-mass shell, and propagators are associated with internal lines.

Each Feynman diagram with n vertices corresponds to $n!$ diagrams of an older version of perturbation theory,²⁻⁴ sometimes referred to as old-fashioned perturbation theory or time-ordered perturbation theory (TOPT). Each of the $n!$ diagrams of TOPT looks like a Feynman diagram with a particular ordering of the vertices; however, the rules are quite different, i.e., the total three-momentum is conserved at each vertex, the intermediate particles are on-the-mass shell, and energy denominators are associated with intermediate states. Also, the integrations that arise with Feynman rules are four dimensional while those of TOPT are three dimensional.

Feynman diagrams are more widely used than TOPT diagrams, because there are fewer of them and they are individually covariant. There have been improvements made on TOPT which make it more attractive. Weinberg⁴ has developed a version of TOPT which has fewer diagrams, while Kadyshevsky⁵ and the author⁶ have reformulated TOPT so that the contributions of individual diagrams to the S matrix are invariant.

Weinberg⁴ arrived at his graphical rules by considering the infinite-momentum limit of TOPT diagrams. More specifically, he studied these diagrams in a Lorentz frame moving at a high velocity in a direction opposite to the total three-momentum \mathbf{P} . In such a frame all particles move with large velocities more or less in the $+\mathbf{P}$ direction. Many of the TOPT diagrams vanish in this limit, and moreover, the energy denominators which occur in the old-fashioned rules are replaced by invariant s denomi-

ators, where $s=P^2$, the square of the total four-momentum. In spite of the appearance of the s denominators, the contributions of individual Weinberg diagrams to the S matrix are not invariant, except in certain special cases.

It has been shown⁷⁻⁹ that the Weinberg infinite-momentum limit can be interpreted as a change of the space-time variables $(x^0, x^1, \mathbf{x}_\perp)$ and the energy-momentum variables $(p^0, p^1, \mathbf{p}_\perp)$ to the light-cone variables $(x_+, x_-, \mathbf{x}_\perp)$ and $(p_-, p_+, \mathbf{p}_\perp)$, where $x_\pm = x^0 \pm x^1$, $p_\pm = p^0 \pm p^1$, and \mathbf{x}_\perp and \mathbf{p}_\perp are transverse with respect to the arbitrarily chosen one axis. In the new variables, x_+ and p_- play the roles of the "time" and "energy," respectively. In this framework it becomes clear¹⁰⁻¹² that the Weinberg rules are related to the front form of relativistic dynamics originally proposed by Dirac,¹³ and that they can be derived by quantizing fields at equal values of t_+ rather than at equal times. For this reason the perturbation theory given by the Weinberg rules, or variations thereof, is often referred to as light front perturbation theory (LFPT).

The connectedness structure of LFPT is similar to that found when TOPT is applied to nonrelativistic problems.⁴ Accordingly, summing series of LFPT diagrams leads to integral equations which are analogous to those encountered in few particle potential problems. Few particle equations which sum series of LFPT diagrams are often called Weinberg equations. The original Weinberg equation⁴ is a light-front ladder approximation for the relativistic two-body problem. Since in LFPT the integrations are three dimensional, Weinberg equations have fewer variables than equations of the Bethe-Salpeter type.^{14,15}

An extensive study of two-body Weinberg equations has been made by Namyslowski and his co-workers.^{16,17} They have introduced a variation of the original light-front variables which involves invariant projections of four-vectors on tetrads, where a tetrad is a set of four mutually orthonormal four-vectors. In contrast to the original

Weinberg equation,⁴ their two-particle equations are manifestly invariant.

Using LFPT, Namyslowski and Weber¹⁷ have examined the effect a disconnected third particle has on a two-particle system. Their results indicate that LFPT can be truncated so as to preserve the cluster property.¹⁸ In this context the cluster property states that the dynamics of a two-body subsystem of a three-body system should be unaffected by the presence of the third particle when interactions with the third particle are negligible.

Other applications of LFPT to two- and three-particle systems have been made in the context of quantum chromodynamics (QCD). An account of the advantages of such an approach to QCD has been given in a series of papers by Brodsky, Lepage, and collaborators.^{19–22} In particular, it has been shown^{19,23} that the nonperturbative, large distance interactions in few-quark systems can be accounted for by turning Weinberg equations into so-called evolution equations.

As mentioned above, LFPT is not the only variation of TOPT. Kadyshevsky⁵ has developed an approach in which an invariant time direction is established by introducing a timelike, unit four-vector, denoted here by λ . This leads to a reformulation of TOPT in which individual diagrams make invariant contributions to the S matrix. The number of diagrams is the same as in TOPT; however, the graphical rules are quite different. Besides the particles described by the underlying quantum fields, there appear so-called quasiparticles or spurions. The total four-momentum of the particles and quasiparticles is conserved at each vertex, the intermediate particles are on-the-mass shell, and propagators are associated with internal lines. The appearance of the quasiparticles makes these diagrams much more complicated than those of Feynman, TOPT, or LFPT.

Recently the author⁶ has shown how to reformulate Kadyshevsky's approach so as to eliminate the quasiparticles. This leads to a covariant version of TOPT whose graphical rules are the same as those of TOPT except for the replacement of three-momentum conserving δ functions by invariant three-dimensional δ functions and the use of invariant denominators rather than energy denominators. The invariants that occur in the denominators are of the type $\lambda \cdot P$, where P is the total four-momentum of a state. This covariant time-ordered perturbation theory (CTOPT) becomes identical to TOPT in a special set of Lorentz frames, called λ frames. A λ frame is one in which $\lambda = (1, 0)$. If λ is chosen parallel to the total four-momentum of the system, a λ frame is the same as a c.m. frame.

In the development of CTOPT the spacelike surfaces given by $\lambda \cdot x = \tau$, where τ is an invariant time parameter, play an important role. It is not difficult to show that in the limit in which the components of λ become infinite, all of these spacelike surfaces become light fronts. This limit is taken by writing $\lambda = (\lambda_0, \lambda)$ and letting $|\lambda| \rightarrow \infty$ subject to the constraint $\lambda^2 = \lambda_0^2 - |\lambda|^2 = 1$.

Here we will see that taking this infinite- λ limit of CTOPT leads to a covariant version of LFPT. The graphical rules for this theory can be stated in a form identical to that given by Weinberg.⁴ The difference lies

in the definition of the variables that are used to label the particle lines. For an on-the-mass shell particle with four-momentum p in a state with total four-momentum P , the original Weinberg variables⁴ are $\eta = p_+ / P_+$ and $q = p_\perp$, while the new definitions are $\eta = \xi \cdot p / \xi \cdot P$ and $q = p_\perp - \eta P_\perp$. Here ξ is a lightlike vector that λ is proportional to in the infinite λ limit. Clearly the η 's are invariants, and we will see that dot products formed from the two-vectors q are also.

The new meaning for the Weinberg variables is important, as it guarantees that the contributions of LFPT diagrams are individually invariant. Also, integral equations obtained by summing series of LFPT diagrams are now manifestly invariant, a highly desirable feature that the original Weinberg equation⁴ lacked.

The infinite- λ limit will be carried out here in the context of a model field theory which describes the interaction of the quanta ψ of a charged scalar field with the quanta ϕ of a neutral scalar field according to the virtual process $\psi \leftrightarrow \psi + \phi$. This model was used⁶ in the development of CTOPT. Since the diagrams for ϕ - ψ scattering are similar to those that arise in models of pion-nucleon scattering in which the elementary virtual processes are $B \leftrightarrow B' + \pi$ ($B, B' = N, \Delta, \dots$), it is of interest to obtain integral equations for ϕ - ψ scattering. Here we will obtain a three-body model for this process by summing all LFPT diagrams with $|\psi\rangle$, $|\psi, \phi\rangle$, and $|\psi, 2\phi\rangle$ intermediate states. We will see that with this model, the amplitudes for $\phi + \psi \rightarrow \phi + \psi$ and $\phi + \psi \rightarrow 2\phi + \psi$ can be obtained by solving a linear, three-dimensional integral equation which, as a result of the use of the new definition of the Weinberg variables, is manifestly invariant. In fact, all of the ingredients of the equation are invariants.

The three-body equations we will develop are similar to those Aaron, Amado, and Young²⁴ derived a number of years ago by imposing two- and three-particle unitarity on a relativistic isobar model, but with some important differences. First of all, the equations developed here look exactly the same in all Lorentz frames, i.e., they are manifestly invariant. It is not only in the c.m. frame that they acquire a concise or practical form. Secondly, they satisfy the cluster property¹⁸ without introducing a spurious singularity in the s variable²⁵ for the three-body system. It has been shown that this singularity is responsible for spurious bound-state solutions,²⁶ so getting rid of it represents more than an aesthetic achievement. As far as this author knows, up until now no one has succeeded in developing invariant, three-dimensional, three-body integral equations which satisfy the cluster property without introducing this spurious s singularity.

The outline of the paper is as follows. In Sec. II the infinite λ limit of CTOPT is taken and it is found that this leads directly to a covariant version of LFPT in terms of the variables (p_+, p_\perp) . It is then shown that transforming to new variables leads to graphical rules just like those of Weinberg. It is demonstrated that the transformation properties of the new variables are such that individual diagrams give invariant contributions to the S matrix. The three-particle equations are derived in Sec. III, and it is verified that they satisfy the cluster property without the occurrence of a spurious singularity in the three-particle s

value. In Sec. IV it is shown that the amplitudes obtained from the three-particle equations satisfy two- and three-particle unitarity. This analysis leads to an expression for the production amplitude which is similar to that assumed in isobar models.²⁴ Finally, Sec. V gives a discussion of the results and suggestions for future work.

II. THE PERTURBATION THEORIES

The various perturbation theories will be analyzed here in the context of a simple field theory which describes the interaction of a neutral scalar particle ϕ with a charged scalar particle ψ by means of the elementary virtual process

$$\psi \rightleftharpoons \psi + \phi. \quad (1)$$

The energies of the particles are given by

$$\omega_k = (\mathbf{k}^2 + \mu^2)^{1/2}, \quad E_p = (\mathbf{p}^2 + m^2)^{1/2}. \quad (2)$$

For the perturbation theories of interest the S matrix for a transition $\alpha \rightarrow \beta$ can be written^{4,6}

$$S_{\beta\alpha} = \delta_{\beta\alpha} - (2\pi)^4 i \delta^4(P_\beta - P_\alpha) \Omega_{\beta\alpha} T_{\beta\alpha}, \quad (3)$$

where P_α and P_β are the total initial and final four-momenta, respectively. The quantity $\Omega_{\beta\alpha}$ is a product of external factors—one for each particle in the initial and final states. The factor for a ψ particle is $(2\pi)^{-3/2}(2E_p)^{-1/2}$, while for a ϕ particle it is $(2\pi)^{-3/2}(2\omega_k)^{-1/2}$. The T -matrix element $T_{\beta\alpha}$ is a Lorentz invariant function of the incoming and outgoing momenta.

The perturbation theories can be summarized in a set of graphical rules for constructing $T_{\beta\alpha}$. The theories differ only in the way the lines are labeled and in the precise form of the various factors. The labels and factors are given in Table I. The CTOPT rules are derived in Ref. 6, while those of LFPT will be obtained here. The general graphical rules are given below.

(a) Draw all possible ordered diagrams for the transition $\alpha \rightarrow \beta$. That is, draw each n th order Feynman diagram $n!$ times, ordering the n vertices in every possible way in a sequence running from right to left, with lines for the particles in the initial state α and the final state β

entering on the right and leaving on the left, respectively. Label each line as indicated in Table I.

(b) Include an internal line factor for each internal line.

(c) For every vertex except the last, include a vertex factor. The factor for the last vertex is already included in (3). Associate a bare coupling constant g_0 with each vertex.

(d) For every intermediate state, i.e., a set of lines between two adjacent vertices, include a denominator factor. In Table I, the intermediate state is indicated by γ .

(e) Integrate the product of these factors over all internal line labels, and sum the result over all diagrams to obtain $T_{\beta\alpha}$.

In CTOPT a timelike unit vector $\lambda = (\lambda_0, \boldsymbol{\lambda})$, with the properties

$$\lambda^2 = 1, \quad \lambda_0 > 0, \quad (4)$$

plays an important role. In particular, it occurs in the definition of the invariant three-dimensional delta function δ_λ that appears in the vertex factors. This δ function is defined by

$$\delta_\lambda(y) \equiv \frac{1}{(2\pi)^3} \int d^4x e^{iy \cdot x} \delta(\lambda \cdot x), \quad (5a)$$

$$= \frac{1}{\lambda_0} \delta^3 \left[\mathbf{y} - \mathbf{y}_0 \frac{\boldsymbol{\lambda}}{\lambda_0} \right], \quad (5b)$$

$$= \delta^3(\mathbf{y}_\lambda). \quad (5c)$$

It follows from (5a) that for any four-vector y , $\delta_\lambda(y)$ is an invariant function of λ and y , i.e., $\delta_\lambda(y) = \delta_{\lambda'}(y')$, where λ' and y' are obtained from λ and y , respectively, by a Lorentz transformation. Integration over x_0 yields (5b). In (5c) \mathbf{y}_λ is the three-vector part of y in a λ frame, i.e., one in which $\lambda = (1, \mathbf{0})$. We will indicate components evaluated in these frames by a subscript λ .

The vertex factors for CTOPT involve $\delta_\lambda(\Delta P)$, where ΔP is the total four-momentum leaving the vertex minus the total four-momentum entering the vertex, with all of the particles on the mass shell. Because of (5c) the total three-momentum in a λ frame is conserved at each vertex.

TABLE I. Labels and factors for the various perturbation theories.

	Covariant time-ordered perturbation theory	Light-front perturbation theory	
		Light-front variables	Weinberg variables
Line labels	\mathbf{p}	(p_+, \mathbf{p}_\perp)	(η, \mathbf{q})
Internal line	$(2\pi)^{-3}(2E_p)^{-1}$	$(2\pi)^{-3}(2p_+)^{-1}\theta(p_+)$	$(2\pi)^{-3}(2\eta)^{-1}\theta(\eta)$
or			
factors	$(2\pi)^{-3}(2\omega_p)^{-1}$		
Vertex factors	$(2\pi)^3 \delta_\lambda(\Delta P)$	$(2\pi)^3 \delta(\Delta P_+) \delta^2(\Delta \mathbf{P}_\perp)$	$(2\pi)^3 \delta(\Delta \Sigma \eta) \delta^2(\Delta \Sigma \mathbf{q})$
Denominator factors	$\frac{1}{\lambda \cdot P_\alpha + i\epsilon - \lambda \cdot P_\gamma}$	$\frac{2}{P_{\alpha-} + i\epsilon - P_{\gamma-}}$	$\frac{2}{s_\alpha + i\epsilon - s_\gamma}$

The denominator factors for CTOPT contain P_α and P_γ , the total four-momentum for the initial and intermediate states, respectively. When the invariant $\lambda \cdot P$ is evaluated in a λ frame, it yields E_λ , the total energy in this frame. Clearly, in a λ frame CTOPT is identical to TOPT. A formal proof that the S matrix calculated with CTOPT is the same as the one obtained from Feynman diagrams is given in Sec. II of Ref. 6. This proof shows that the S matrix is independent of the arbitrary external vector λ , which is a necessary requirement for covariance.

In order to illustrate the CTOPT rules and to make a couple of important points, we give below the contribution to the T matrix which arises from the diagram in Fig. 1.

$$g_0^2 \int \frac{d^3 p''}{(2\pi)^3 2E_{p''}} \frac{(2\pi)^3 \delta_\lambda(P_\alpha + p'')}{\lambda \cdot P_\alpha + i\epsilon - \lambda \cdot (P_\beta + p'' + P_\alpha)} . \quad (6a)$$

where

$$P_\alpha = p + k, \quad P_\beta = p' + k'. \quad (6b)$$

It is important to note that in the diagrams we deal with here, all of the lines flow from right to left, i.e., in contrast to Feynman diagrams we do not imagine that the p'' line in Fig. 1 is flowing "backwards in time."

The integration in (6a) can be easily carried out by using (5c) and the fact that $d^3 p''/E_{p''}$ is an invariant. We do not bother to give the result, but do point out that because of the δ_λ function,

$$\mathbf{P}_{\alpha\lambda} = \mathbf{P}_{\gamma\lambda} = \mathbf{P}_{\beta\lambda}, \quad (7)$$

where $\mathbf{P}_{\gamma\lambda}$ is the λ frame total three-momentum in the intermediate state, i.e., $\mathbf{P}_{\gamma\lambda} = \mathbf{P}_{\alpha\lambda} + \mathbf{p}''_\lambda + \mathbf{P}_{\beta\lambda}$. The fact that the λ -frame total three-momentum is the same in every state (initial, intermediate, and final) is a general feature of CTOPT.

We will now show that the rules of LFPT can be obtained by parametrizing λ in the form

$$\lambda = (\cosh \rho, -\hat{\mathbf{u}} \sinh \rho), \quad (8)$$

$$\rho > 0, \quad \hat{\mathbf{u}} \cdot \hat{\mathbf{u}} = 1,$$

and letting $\rho \rightarrow \infty$. That this limit should lead to LFPT can be seen quite simply. In TOPT the spacelike surfaces $t = \text{const}$ play a privileged rule, while in CTOPT these

surfaces are replaced by the spacelike surfaces $\lambda \cdot x = \tau$, where τ is an invariant time parameter. When $\rho \rightarrow \infty$, the spacelike surfaces become light fronts.

By using (8) and the Lorentz transformation from a general frame to a λ frame [Eqs. (30) of Ref. 6], we can write

$$p_{0\lambda} = \frac{1}{2}(e^\rho p_+ + e^{-\rho} p_-) = \lambda \cdot p, \quad (9)$$

$$\hat{\mathbf{u}} \cdot \mathbf{p}_\lambda = \frac{1}{2}(e^\rho p_+ - e^{-\rho} p_-), \quad (10)$$

$$\mathbf{p}_{\lambda\perp} = \mathbf{p}_\perp, \quad (11)$$

where p is any four-momentum and we have introduced the notation

$$A_\pm = A_0 \pm \mathbf{A} \cdot \hat{\mathbf{u}}, \quad (12)$$

$$\mathbf{A}_\perp = \mathbf{A} - \mathbf{A} \cdot \hat{\mathbf{u}} \hat{\mathbf{u}}. \quad (13)$$

Combining (9) and (10), we find

$$\lambda \cdot P = \hat{\mathbf{u}} \cdot \mathbf{P}_\lambda + e^{-\rho} P_-, \quad (14)$$

with

$$P = \sum_n p_n, \quad (15)$$

$$\mathbf{P}_\lambda = \sum_n \mathbf{p}_{n\lambda}, \quad (16)$$

$$P_\pm = \sum_n p_{n\pm}, \quad (17)$$

where the sums are over all particles in a state (initial, intermediate, or final). From (7) and (14) it follows that for the denominator factor of CTOPT we have

$$\lambda \cdot P_\alpha - \lambda \cdot P_\gamma = e^{-\rho}(P_{\alpha-} - P_{\gamma-}). \quad (18)$$

According to (5c), (10), and (11), we can write

$$\delta_\lambda(\Delta P) = 2e^{-\rho} \delta[\Delta(P_+ - e^{-2\rho} P_-)] \delta^2(\Delta \mathbf{P}_\perp), \quad (19)$$

where ΔP_\pm and $\Delta \mathbf{P}_\perp$ are the changes in the plus-minus and transverse components of the total four-momentum at a vertex. In the N th order of perturbation theory, we have $N-1$ vertex factors and $N-1$ sets of intermediate states, so the $e^{-\rho}$ factors in (18) and (19) cancel out. Upon letting $\rho \rightarrow \infty$, we obtain the vertex and denominator factors in the second column of Table I.

From the arguments of the new vertex factors it is clear that the natural variables are (p_+, \mathbf{p}_\perp) . The integrations can be easily transformed from $\mathbf{p} = (\mathbf{p} \cdot \hat{\mathbf{u}}, \mathbf{p}_\perp)$ to (p_+, \mathbf{p}_\perp) by using

$$p_+ = [(\mathbf{p} \cdot \hat{\mathbf{u}})^2 + \mathbf{p}_\perp^2 + m^2]^{1/2} + \mathbf{p} \cdot \hat{\mathbf{u}}, \quad (20a)$$

$$d^3 p / E_p = dp_+ d^2 p_\perp / p_+. \quad (20b)$$

According to (20a) p_+ must lie in the interval $(0, \infty)$, which accounts for the step function $\theta(p_+)$ in the internal line factors. This completes the justification for the entries in the second column of Table I.

It should be noted that in computing the denominator factors we can express the minus component of a particle's momentum in terms of its plus and transverse components by using

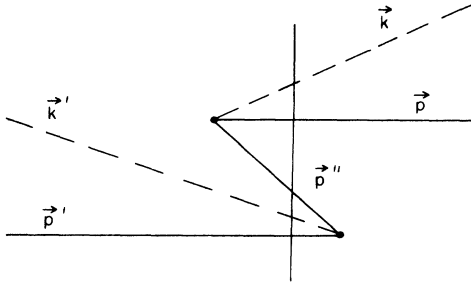


FIG. 1. A contribution to ϕ - ψ scattering in CTOPT.

$$p_{n-} = \frac{\mathbf{p}_{n\perp}^2 + m_n^2}{p_{n+}}, \quad (21)$$

which follows from (12) and (13) and the fact that the particles are on the mass shell. Also, since the plus and transverse components of the momentum are conserved at each vertex, we have

$$P_{\alpha+} = P_{\gamma+} = P_{\beta+} \equiv P_+, \quad (22a)$$

$$\mathbf{P}_{\alpha\perp} = \mathbf{P}_{\gamma\perp} = \mathbf{P}_{\beta\perp} \equiv \mathbf{P}_\perp, \quad (22b)$$

where α , β , and γ refer to the initial, the final, and any intermediate state, respectively. We see that the conservation of the total λ -frame three-momentum in CTOPT has been replaced in LFPT by the conservation of the plus and transverse components of the total four-momentum.

In order to obtain the entries in the third column of Table I, we introduce variables η and \mathbf{q} that are covariant generalizations of the variables introduced some time ago by Weinberg.⁴ We define for each particle

$$\eta = p_+ / P_+, \quad (23a)$$

$$= \xi \cdot p / \xi \cdot P, \quad (23b)$$

where ξ is the lightlike vector

$$\xi = \xi_0(1, -\hat{\mathbf{u}}), \quad (24)$$

and

$$\mathbf{q} = \mathbf{p}_\perp - \eta \mathbf{P}_\perp. \quad (25)$$

It is important to keep in mind that P_+ and \mathbf{P}_\perp are fixed throughout any process [see (22)], and therefore

$$\sum_n \eta_n = 1, \quad (26a)$$

$$\sum_n \mathbf{q}_n = 0, \quad (26b)$$

where the sums are over all of the particles in a state (initial, final, or intermediate).

From (12) and (13) it follows that the scalar product of any two four-vectors can be written in the form

$$A \cdot B = \frac{1}{2}(A_+ B_- + A_- B_+) - \mathbf{A}_\perp \cdot \mathbf{B}_\perp. \quad (27)$$

Using this, (23a), and (25), we find

$$\mathbf{q} \cdot \mathbf{q}' = -(p - \eta P) \cdot (p' - \eta' P'), \quad (28)$$

where (η, \mathbf{q}) and (η', \mathbf{q}') are the variables for the particles whose four-momenta are p and p' , while P and P' are the total four-momenta for the states (initial, intermediate, or final) in which these particles occur. It should be noted that the particles can occur in different states. According to (23b) and (28), η and $\mathbf{q} \cdot \mathbf{q}'$ are invariants.

From (28), (26a), and (15), it follows that

$$\frac{\mathbf{q}^2 + m^2}{\eta} = 2p \cdot P - \eta s \quad (29)$$

and

$$\sum_n \frac{\mathbf{q}_n^2 + m_n^2}{\eta_n} = s, \quad (30)$$

where s is the square of the total energy in the c.m. system for the state of interest, and is given by

$$s = P^2. \quad (31)$$

The sum in (30) is over all the particles in the state.

Using (27), (22), (23a), and (25), we find

$$s_\alpha - s_\gamma = P_+ (P_{\alpha-} - P_{\gamma-}) \quad (32)$$

and

$$\delta(\Delta \Sigma \eta) \delta^2(\Delta \Sigma \mathbf{q}) = P_+ \delta(\Delta P_+) \delta^2(\Delta \mathbf{P}_\perp), \quad (33)$$

where $\Delta \Sigma \eta$ and $\Delta \Sigma \mathbf{q}$ represent the changes in the total η and total \mathbf{q} at a vertex. Since there are as many denominator factors in a diagram as there are vertex factors, the P_+ 's in (32) and (33) cancel out. Integrals can be transformed from the (p_+, \mathbf{p}_\perp) variables to the (η, \mathbf{q}) variables by using

$$dp_+ d^2 p_\perp / p_+ = d\eta d^2 q / \eta, \quad (34)$$

$$\theta(p_+) = \theta(\eta). \quad (35)$$

This completes the justification for the entries in the third column of Table I.

We conclude this section by emphasizing an important feature of LFPT. In Fig. 1, conservation of the η 's and (26a) require that for the \mathbf{p}'' particle, $\eta'' = -1$; however, the step function $\theta(\eta'')$ forbids this, and therefore the diagram makes no contribution to the S matrix. In general, diagrams give no contribution whenever a vertex has lines coming in from the right, but has no lines going out to the left, or vice versa. This is so because η conservation requires that the sum of the η 's of these lines vanish, and this is forbidden by the requirement that all η 's be positive.

III. THREE PARTICLE EQUATIONS

In this section we will derive a set of three-particle equations for ϕ - ψ scattering which, since the basic interaction is (1), can be thought of as an analog of pion-nucleon scattering. The equations will be obtained by summing all diagrams with $|\psi\rangle$, $|\psi, \phi\rangle$, and $|\psi, 2\phi\rangle$ intermediate states.

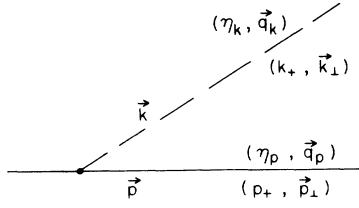
In order to make the equations more general and to alleviate convergence problems with the integrals, we will assign a cutoff function to the vertex shown in Fig. 2. In this figure we show all three labels for each of the particles (see Table I). The graphical rules with the cutoff function are the same as those given in Sec. II, except for the replacement of the bare coupling constant according to

$$g_0 \rightarrow g_0(\xi, \rho), \quad (36)$$

with

$$\xi = \frac{k_+}{k_+ + p_+} \quad (37a)$$

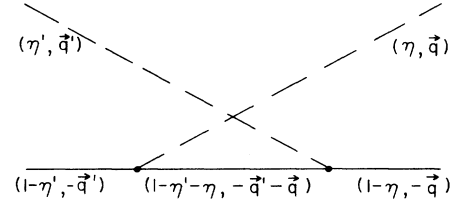
$$= \frac{\eta_k}{\eta_k + \eta_p}, \quad (37b)$$

FIG. 2. The ϕ - ψ vertex.

$$\rho = \mathbf{k}_\perp - \zeta(\mathbf{k}_\perp + \mathbf{p}_\perp) \quad (37c)$$

$$= \frac{\eta_p \mathbf{q}_k - \eta_k \mathbf{q}_p}{\eta_k + \eta_p}, \quad (37d)$$

where (37b) and (37d) are obtained with the aid of (23a) and (25). We will see that the assumption that the cutoff function depends only on the momenta through ζ and ρ preserves the cluster property. Furthermore, since the η 's and dot products of the \mathbf{q} 's are Lorentz invariants, we will assume that the cutoff actually only depends on ζ and ρ^2 , thereby making it an invariant function. We will continue to denote it, however, as in (36). By following the analysis

FIG. 3. A crossed Born term for ϕ - ψ scattering.

that leads to (30), it is straightforward to show that

$$\frac{\rho^2 + \mu^2}{\zeta} + \frac{\rho^2 + m^2}{1 - \zeta} = 2m^2 + 2\mu^2 - (p - k)^2, \quad (38)$$

so we can, if so desired, write the cutoff as a function of $(p - k)^2$.

We begin summing diagrams by considering only those with $|\psi, \phi\rangle$ and $|\psi, 2\phi\rangle$ intermediate states, i.e., we ignore the one- ψ reducible diagrams for now. Within this set the lowest order diagram is given by Fig. 3. Using the LFPT rules with the Weinberg variables, we find its contribution to be

$$B_0(\eta', \mathbf{q}'; \eta, \mathbf{q}; s) = \frac{\theta(1 - \eta' - \eta)}{1 - \eta' - \eta} \frac{g_0 \left[\frac{\eta}{1 - \eta'}, \mathbf{q} + \frac{\eta}{1 - \eta'} \mathbf{q}' \right] g_0 \left[\frac{\eta'}{1 - \eta}, \mathbf{q}' + \frac{\eta'}{1 - \eta} \mathbf{q} \right]}{s - s_3(\eta', \mathbf{q}'; \eta, \mathbf{q})}, \quad (39a)$$

with

$$s_3(\eta', \mathbf{q}'; \eta, \mathbf{q}) = \frac{\mathbf{q}'^2 + \mu^2}{\eta'} + \frac{(\mathbf{q}' + \mathbf{q})^2 + m^2}{1 - \eta' - \eta} + \frac{\mathbf{q}^2 + \mu^2}{\eta}, \quad (39b)$$

where s_3 is the s value for the $|\psi, 2\phi\rangle$ intermediate state. Here, and in what follows, we assume that s , without any subscript, is a free complex parameter, unless stated otherwise. In particular, we do not identify it with the initial state s value as in Table I. This will give us a completely “off-shell” theory.

It should be noted that the diagram obtained by reversing the order of the vertices in Fig. 3 has three ψ particles in the intermediate state and hence an s value whose lower bound is $(3m)^2$. Since $s_3 \geq (2\mu + m)^2$, it is reasonable to assume that the diagram with the opposite ordering to Fig. 3 is negligible at low and intermediate energies if we assume that μ and m are the pion and nucleon mass, respectively.

Applying the graphical rules to Fig. 4, we find the contribution

$$\frac{1}{2(2\pi)^3} \int d\eta'' d^2 q'' \frac{\theta(\eta'') \theta(1 - \eta'')}{\eta''(1 - \eta'')} \frac{B_0(\eta', \mathbf{q}'; \eta'', \mathbf{q}''; s) B_0(\eta'', \mathbf{q}''; \eta, \mathbf{q}; s)}{s - s_2(\eta'', \mathbf{q}'')}, \quad (40a)$$

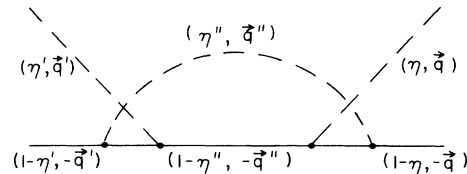
with

$$s_2(\eta, \mathbf{q}) = \frac{\mathbf{q}^2 + \mu^2}{\eta} + \frac{\mathbf{q}^2 + m^2}{1 - \eta}, \quad (40b)$$

where s_2 is the s value for the $|\psi, \phi\rangle$ intermediate state.

It is now obvious how to sum the series of diagrams in Fig. 5. This series leads to a two-particle integral equation with the potential given by (39) and the propagator identified from (40) as

$$(1 - \eta)^{-1} [s - s_2(\eta, \mathbf{q})]^{-1}.$$

FIG. 4. A fourth order contribution to ϕ - ψ scattering.

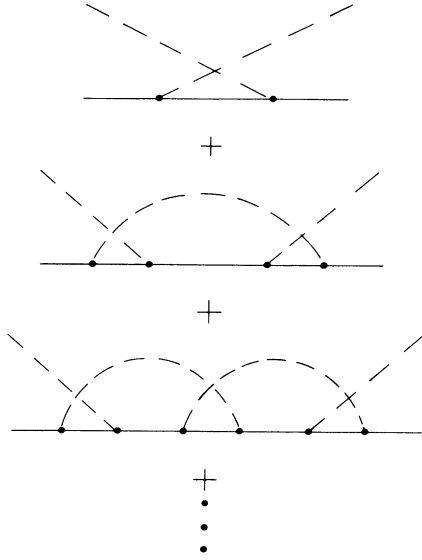


FIG. 5. A series of one- ψ irreducible diagrams for ϕ - ψ scattering.

In order to obtain a three-particle theory, we must include diagrams such as Fig. 6. This leads us to consider the series of diagrams in Fig. 7, which gives the dressing of the ψ particle in the so-called "chain approximation."¹⁵ We find

$$\begin{aligned} \frac{Z}{D(s)} &= \frac{1}{s - m_0^2} + \frac{\Sigma(s)}{(s - m_0^2)^2} + \frac{\Sigma^2(s)}{(s - m_0^2)^3} + \cdots \\ &= [s - m_0^2 - \Sigma(s)]^{-1}, \end{aligned} \quad (41)$$

where $D(s)$ is the renormalized ψ propagator, Z is a renormalization constant to be determined, m_0 is the bare ψ mass, and $\Sigma(s)$ is the self-energy, which in our approximation is given by

$$\Sigma(s) = \frac{1}{2(2\pi)^3} \int d\eta d^2q \frac{\theta(\eta)\theta(1-\eta)}{\eta(1-\eta)} \frac{g_0^2(\eta, \mathbf{q})}{s - s_2(\eta, \mathbf{q})}. \quad (42)$$

It should be noted that in order to obtain sensible results at our level of approximation we must use the physical ψ mass m in the expression for $\Sigma(s)$. It is interesting to observe that (42) is also obtained if we use the Feynman rules, since in LFPT the diagram with the other ordering

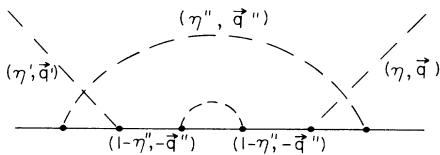


FIG. 6. A diagram that contributes to the dressing of an intermediate ψ particle.

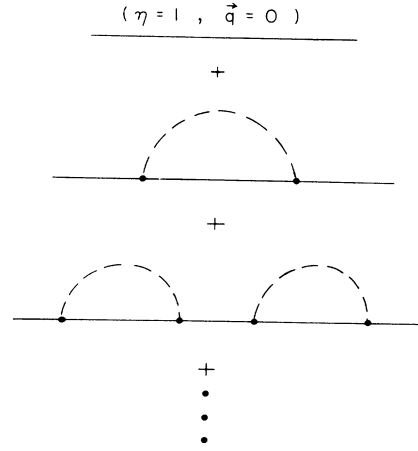


FIG. 7. Chain approximation for the ψ propagator.

of the two vertices makes no contribution.

In order to determine the parameters Z and m_0 we can proceed in exact analogy to the renormalization of the Lee model.³ From (42) and (40b), it follows that $\Sigma(s)$ is a real, analytic function of s with a right-hand cut (RHC) for real $s \geq (\mu + m)^2$, so, for real $s \leq (\mu + m)^2$, $\Sigma(s)$ is a real monotonic function of s . By choosing m_0 small enough we can always find a solution³ of

$$D(m^2) = 0. \quad (43)$$

Assuming this is so, we can choose Z so that

$$D(s) \xrightarrow{s \rightarrow m^2} s - m^2, \quad (44)$$

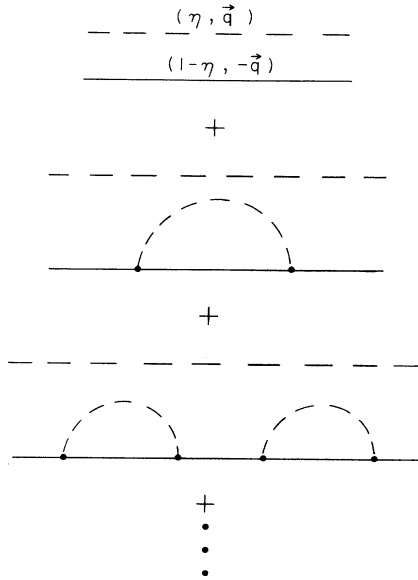


FIG. 8. Chain approximation for the ψ propagator in the presence of a noninteracting ϕ particle.

which leads to

$$Z^{-1} = 1 - \Sigma'(m^2) > 1. \quad (45)$$

Now we consider the series of diagrams in Fig. 8 which describe the dressing of the ψ particle in the presence of a noninteracting ϕ particle. We find a series just like (41)

but with $(s - m_0^2)^{-1}$ replaced by

$$\frac{1}{1-\eta} \frac{1}{s - s_2(\eta, \mathbf{q})} = \frac{1}{(P-k)^2 - m^2} \quad (46)$$

with $m \rightarrow m_0$, and $\Sigma(s)$ replaced by

$$\frac{1}{2(2\pi)^3} \int d\eta' d^2q' \frac{\theta(\eta')\theta(1-\eta-\eta')}{\eta'(1-\eta-\eta')} \frac{g_0^2 \left[\frac{\eta'}{1-\eta}, \mathbf{q}' + \frac{\eta'}{1-\eta} \mathbf{q} \right]}{s - s_3(\eta, \mathbf{q}; \eta', \mathbf{q}')} = \Sigma[(P-k)^2], \quad (47)$$

where

$$s = P^2 = P_+ P_- - \mathbf{P}_\perp^2, \quad (48a)$$

$$k_+ = \eta P_+, \quad \mathbf{k}_\perp = \mathbf{q} + \eta \mathbf{P}_\perp, \quad k_- = \frac{\mathbf{k}_\perp^2 + \mu^2}{k_+}. \quad (48b)$$

It seems intuitively clear that the equalities in (46) and (47) are valid, but it is important to verify them as they indicate that truncations of LCPT do not violate the cluster property. To verify (46) we only need to use (27) and (48). We can verify (47) by making the transformations

$$\eta'' = \frac{\eta'}{1-\eta}, \quad (49a)$$

$$\mathbf{q}'' = \mathbf{q}' + \frac{\eta'}{1-\eta} \mathbf{q}, \quad (49b)$$

assuming $0 < \eta < 1$, and comparing with (42).

We are now in a position to sum all diagrams with $|\psi, \phi\rangle$ and $|\psi, 2\phi\rangle$ intermediate states. We find that this sum is given by the iterative solution of an equation which can be written symbolically as

$$Y_0 = B_0 + B_0 \frac{Z}{D} Y_0. \quad (50)$$

We renormalize the quantities that occur in this equation as follows:

$$Y(\eta', \mathbf{q}'; \eta, \mathbf{q}; s) = Z Y_0(\eta', \mathbf{q}'; \eta, \mathbf{q}; s), \quad (51)$$

$$B(\eta', \mathbf{q}'; \eta, \mathbf{q}; s) = Z B_0(\eta', \mathbf{q}'; \eta, \mathbf{q}; s), \quad (52)$$

$$g(\zeta, \rho) = Z^{1/2} g_0(\zeta, \rho). \quad (53)$$

This takes account of the renormalization of external lines and the coupling constant. Our approximate equation for the one- ψ irreducible ϕ - ψ amplitude is then given by

$$Y(\eta', \mathbf{q}'; \eta, \mathbf{q}; s) = B(\eta', \mathbf{q}'; \eta, \mathbf{q}; s) + \frac{1}{2(2\pi)^3} \int_0^1 \frac{d\eta''}{\eta''} \int d^2q'' \frac{B(\eta', \mathbf{q}'; \eta'', \mathbf{q}''; s) Y(\eta'', \mathbf{q}''; \eta, \mathbf{q}; s)}{D[(P-k'')^2 + i\epsilon]}, \quad s = P^2 + i\epsilon, \quad (54)$$

where

$$(P-k'')^2 = (1-\eta'') \left[s - \frac{\mathbf{q}''^2 + \mu^2}{\eta''} \right] - \mathbf{q}''^2. \quad (55)$$

It is important to note that this equation satisfies the cluster property without introducing the spurious singularity^{25,26} in s that occurs in other relativistic three-particle equations.

Our job is now to find the contribution of the one- ψ reducible diagrams to the ϕ - ψ amplitude. The series of diagrams we are summing is topologically equivalent to the series that arises in finding the θ - V amplitude in an extension of the Lee model²⁷ in which the elementary processes are $V \rightleftharpoons N + \theta$ and $W \rightleftharpoons V + \theta$, where V , N , and W are fermions and θ is a scalar boson. The one- W reducible diagrams in this extended Lee model are topologically equivalent to the one- ψ reducible diagrams under consideration here. The analysis of Ref. 27 shows that we can take account of these processes by adding to the potential B in (54) the separable potential

$$W(\eta', \mathbf{q}'; \eta, \mathbf{q}; s) = \frac{g(\eta', \mathbf{q}') g(\eta, \mathbf{q})}{s - m_0^2}. \quad (56)$$

Our complete ϕ - ψ amplitude is then given by the solution of the equation

$$X(\eta', \mathbf{q}'; \eta, \mathbf{q}; s) = V(\eta', \mathbf{q}'; \eta, \mathbf{q}; s) + \frac{1}{2(2\pi)^3} \int_0^1 \frac{d\eta''}{\eta''} \int d^2 q'' \frac{V(\eta', \mathbf{q}'; \eta'', \mathbf{q}''; s) X''(\eta'', \mathbf{q}''; \eta, \mathbf{q}; s)}{D[(P - k'')^2 + i\epsilon]}, \quad s = P^2 + i\epsilon, \quad (57)$$

where

$$V(\eta', \mathbf{q}'; \eta, \mathbf{q}; s) = B(\eta', \mathbf{q}'; \eta, \mathbf{q}; s) + W(\eta', \mathbf{q}'; \eta, \mathbf{q}; s). \quad (58)$$

As a result of the separability of W it is not difficult to separate the one- ψ irreducible and one ψ -reducible contributions to X . The manipulations are identical to those given in Sec. VII of Ref. 28. The result is

$$X(\eta', \mathbf{q}'; \eta, \mathbf{q}; s) = Y(\eta', \mathbf{q}'; \eta, \mathbf{q}; s) + \frac{\gamma(\eta', \mathbf{q}'; s) \gamma(\eta, \mathbf{q}; s)}{\tilde{D}(s)}, \quad (59)$$

where

$$\gamma(\eta, \mathbf{q}; s) \tilde{Z}^{-1/2} = g(\eta, \mathbf{q}) + \frac{1}{2(2\pi)^3} \int_0^1 \frac{d\eta'}{\eta'} \int d^2 q' \frac{Y(\eta, \mathbf{q}; \eta', \mathbf{q}'; s) g(\eta', \mathbf{q}')}{D[(P - k')^2 + i\epsilon]}, \quad s = P^2 + i\epsilon, \quad (60)$$

$$\tilde{D}(s) \tilde{Z}^{-1} = s - m_0^2 - \tilde{\Sigma}(s), \quad (61)$$

$$\begin{aligned} \tilde{\Sigma}(s) = & \frac{1}{2(2\pi)^3} \int_0^1 \frac{d\eta'}{\eta'} \int d^2 q' \frac{1}{2(2\pi)^3} \int_0^1 \frac{d\eta}{\eta} \int d^2 q g(\eta', \mathbf{q}') \\ & \times \left\{ 2(2\pi)^3 \eta \frac{\delta(\eta' - \eta) \delta^2(\mathbf{q}' - \mathbf{q})}{D[(P - k)^2 + i\epsilon]} \right. \\ & \left. + \frac{Y(\eta', \mathbf{q}'; \eta, \mathbf{q}; s)}{D[(P - k')^2 + i\epsilon] D[(P - k)^2 + i\epsilon]} \right\} g(\eta, \mathbf{q}). \end{aligned} \quad (62)$$

The parameters \tilde{Z} and m_0 are determined by

$$\tilde{D}(s) \xrightarrow{s \rightarrow m^2} s - m^2. \quad (63)$$

It is not difficult to show that $\tilde{\Sigma}(s)$ sums the diagrams of Fig. 9; thus it represents an approximation to the ψ self-energy which includes the effect of $|\psi, \phi\rangle$ and $|\psi, 2\phi\rangle$ intermediate states. In other words $1/\tilde{D}(s)$ is the ψ propagator calculated at the three-particle level of approximation. The vertex function $\gamma(\eta, \mathbf{q}; s)$ also includes the effect of all $|\psi, \phi\rangle$ and $|\psi, 2\phi\rangle$ intermediate states. Some typical diagrams that are included are shown in Fig. 10.

IV. UNITARY AND THE PRODUCTION AMPLITUDE

Here we shall sketch how the unitarity relations for the ϕ - ψ amplitude can be derived directly from the integral equation (57). It is important to verify that this equation, which is based on a truncation of LFPT, leads to solutions which

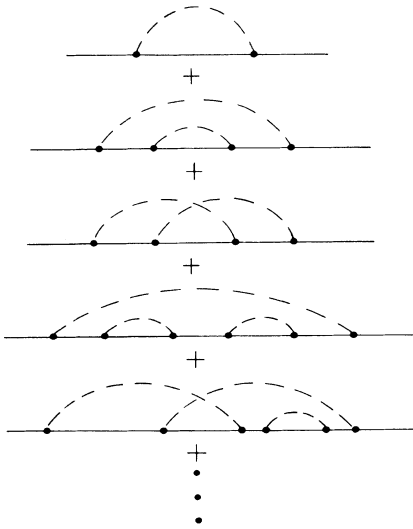


FIG. 9. Contributions to the ψ self-energy.

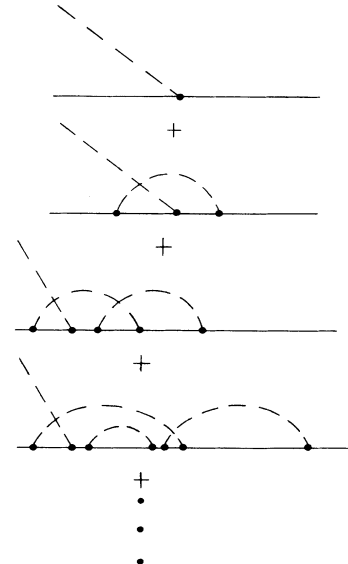


FIG. 10. Contributions to the vertex function.

satisfy two- and three-particle unitarity exactly. This verification will also give us an expression for the $\psi + \phi \rightarrow \psi + 2\phi$ production amplitude.

We will see that the solution of (57) has a RHC for real $s \geq (\mu + m)^2$. This cut arises because of cuts in $1/D(s)$ and $V(\eta', \mathbf{q}'; \eta, \mathbf{q}; s)$. We recall that $1/D(s)$ has a simple pole with unit residue at $s = m^2$ as well as a RHC for real $s \geq (\mu + m^2)$ [see (44) and (42)]. Using this, (55), (40b), (41), (47), and (53), we can show that

$$\begin{aligned} \text{disc} \frac{1}{D[(P-k)^2]} &= \frac{1}{D[(P-k)^2 + i\epsilon]} - \frac{1}{D[(P-k)^2 - i\epsilon]} \\ &= -\frac{2\pi i}{1-\eta} \delta[s - s_2(\eta, \mathbf{q})] - \frac{2\pi i}{D[(P-k)^2 + i\epsilon]D[(P-k)^2 - i\epsilon]} \frac{1}{2(2\pi)^3} \\ &\quad \times \int d\eta' d^2q' \frac{\theta(\eta')\theta(1-\eta-\eta')}{\eta'(1-\eta-\eta')} g^2 \left[\frac{\eta'}{1-\eta}, \mathbf{q}' + \frac{\eta'}{1-\eta} \mathbf{q} \right] \delta[s - s_3(\eta', \mathbf{q}'; \eta, \mathbf{q})] . \end{aligned} \quad (64)$$

From (39), (52), (53), and (58), we find

$$\begin{aligned} \text{disc} V(\eta', \mathbf{q}'; \eta, \mathbf{q}; s) &= -2\pi i \frac{\theta(1-\eta'-\eta)}{1-\eta'-\eta} g \left[\frac{\eta'}{1-\eta}, \mathbf{q}' + \frac{\eta'}{1-\eta} \mathbf{q} \right] g \left[\frac{\eta}{1-\eta'}, \mathbf{q} + \frac{\eta}{1-\eta'} \mathbf{q}' \right] \\ &\quad \times \delta[s - s_3(\eta', \mathbf{q}'; \eta, \mathbf{q})] , \end{aligned} \quad (65)$$

where we have assumed the singularity in W is outside the range of interest. It can be shown²⁷ that in any case this singularity does not contribute to the discontinuity in X .

Since s_2 and s_3 are the s values for the $|\psi, \phi\rangle$ and $|\psi, 2\phi\rangle$ intermediate states, we have

$$s_2 \geq (\mu + m)^2, \quad s_3 \geq (2\mu + m)^2, \quad (66)$$

thus the first term on the right-hand side of (64) gives rise to the two-particle cut in X , while the second term, as well as (65), lead to the three-particle cut in X .

Not only does $\text{disc} V$ vanish when s is below the ψ - 2ϕ threshold, but also when s is “on-shell.” This can be seen as follows. By using (27) it is straightforward to show that

$$(1-\eta'-\eta)[s - s_3(\eta', \mathbf{q}'; \eta, \mathbf{q})] = (p' - k)^2 - m^2, \quad s = s_2(\eta', \mathbf{q}') \quad (67a)$$

$$= (p - k')^2 - m^2, \quad s = s_2(\eta, \mathbf{q}), \quad (67b)$$

where k is given by (48b) and p is given by

$$p_+ = (1-\eta)P_+, \quad \mathbf{p}_\perp = -\mathbf{q} + (1-\eta)\mathbf{P}_\perp, \quad p_- = \frac{\mathbf{p}_\perp^2 + m^2}{P_+}, \quad (68)$$

with similar expressions for k' and p' . It is elementary to show that the right-hand sides of (67a) and (67b) cannot vanish, so

$$\text{disc} V(\eta', \mathbf{q}'; \eta, \mathbf{q}; s) = 0, \quad (69)$$

when

$$s = s_2(\eta', \mathbf{q}') \quad \text{or} \quad s = s_2(\eta, \mathbf{q}). \quad (70)$$

By using the procedure given in Sec. VI of Ref. 28, it is not difficult to show that when both relations in (70) are satisfied, we have

$$\begin{aligned} \text{disc} X(\eta', \mathbf{q}'; \eta, \mathbf{q}; s) &= \int_0^1 \frac{d\eta''}{\eta''} \int \frac{d^2q''}{2(2\pi)^3} \int_0^1 \frac{d\eta'''}{\eta'''} \int \frac{d^2q'''}{2(2\pi)^3} X(\eta', \mathbf{q}'; \eta'', \mathbf{q}''; s \pm i\epsilon) \\ &\quad \times \left\{ 2(2\pi)^3 \eta'' \delta(\eta'' - \eta''') \delta^2(\mathbf{q}'' - \mathbf{q}''') \right. \\ &\quad \times \text{disc} \frac{1}{D[(P-k'')^2]} + \frac{\text{disc} V(\eta'', \mathbf{q}''; \eta''', \mathbf{q}'''; s)}{D[(P-k'')^2 \pm i\epsilon]D[(P-k''')^2 \pm i\epsilon]} \left. \right\} \\ &\quad \times X(\eta''', \mathbf{q}'''; \eta, \mathbf{q}; s \mp i\epsilon), \quad s = P^2. \end{aligned} \quad (71)$$

By looking at the iterations of (57) it is easy to see that

$$X^*(\eta, \mathbf{q}; \eta', \mathbf{q}'; s^*) = X(\eta', \mathbf{q}'; \eta, \mathbf{q}; s) = X(\eta, \mathbf{q}; \eta', \mathbf{q}'; s), \quad (72)$$

which when used in conjunction with the real, analytic character of $D(s)$ as well as (64) and (65), leads to

$$\begin{aligned} \text{Im} X(\eta', \mathbf{q}'; \eta, \mathbf{q}; s) &= -\pi \int_0^1 \frac{d\eta''}{\eta''} \int \frac{d^2 q''}{2(2\pi)^3} \frac{\delta[s - s_2(\eta'', \mathbf{q}'')] }{1 - \eta''} X^*(\eta'', \mathbf{q}''; \eta', \mathbf{q}'; s + i\epsilon) X(\eta'', \mathbf{q}''; \eta, \mathbf{q}; s + i\epsilon) \\ &\quad - \pi \int_0^1 \frac{d\eta''}{\eta''} \int \frac{d^2 q''}{2(2\pi)^3} \int_0^1 \frac{d\eta'''}{\eta'''} \int \frac{d^2 q'''}{2(2\pi)^3} \frac{\theta(1 - \eta'' - \eta''')}{1 - \eta'' - \eta'''} \frac{1}{2} \delta[s - s_3(\eta'', \mathbf{q}''; \eta''', \mathbf{q}''')] \\ &\quad \times T^*(\eta'', \mathbf{q}'', \eta''', \mathbf{q}'''; \eta', \mathbf{q}'; s + i\epsilon) T(\eta'', \mathbf{q}'', \eta''', \mathbf{q}'''; \eta, \mathbf{q}; s + i\epsilon), \quad s = P^2. \end{aligned} \quad (73)$$

The production amplitude T is given by

$$T(\eta'', \mathbf{q}'', \eta''', \mathbf{q}'''; \eta, \mathbf{q}; s) = F(\eta'', \mathbf{q}'', \eta''', \mathbf{q}'''; \eta, \mathbf{q}; s) + F(\eta''', \mathbf{q}'''; \eta'', \mathbf{q}''; \eta, \mathbf{q}; s), \quad (74)$$

with

$$F(\eta'', \mathbf{q}'', \eta''', \mathbf{q}'''; \eta, \mathbf{q}; s + i\epsilon) = g \left[\frac{\eta''}{1 - \eta'''} \mathbf{q}'' + \frac{\eta'''}{1 - \eta''} \mathbf{q}''' \right] \frac{X(\eta''', \mathbf{q}'''; \eta, \mathbf{q}; s + i\epsilon)}{D[(P - k''')^2 + i\epsilon]}, \quad s = P^2. \quad (75)$$

Here (η'', \mathbf{q}'') and (η''', \mathbf{q}''') refer to the ϕ particles in the final $|\psi, 2\phi\rangle$ state.

Equation (73) is the unitarity relation for the ϕ - ψ elastic scattering amplitude. Because it is written in terms of the Weinberg variables, it may look a little unfamiliar; however, it can easily be brought to the standard form¹⁵ by transforming back to ordinary momentum variables. Finally, the expression for the production amplitude given by (74) and (75) can be checked by summing the diagrams for $\phi + \psi \rightarrow 2\phi + \psi$ in which only $|\psi\rangle$, $|\psi, \phi\rangle$, and $|\psi, 2\phi\rangle$ intermediate states occur. The production amplitude has the form *assumed* in an isobar model.²⁴

V. DISCUSSION

We have shown that it is possible to obtain the graphical rules of LFPT by taking a limit other than the infinite momentum limit of Weinberg.⁴ The limit we have taken involves the unit four-vector λ which provides the invariant time direction for CTOPT.⁶ In the infinite λ limit the spacelike surfaces $\lambda \cdot x = \tau$, where τ is an invariant time parameter, all become light fronts. Since CTOPT is manifestly covariant, this limit gives a manifestly covariant version of LEPT. This is in contrast to Weinberg's original version⁴ of LFPT which was obtained as a limit of TOPT.

It is worth noting that the LFPT obtained here can be derived in a somewhat different manner. As pointed out previously, CTOPT reduces to TOPT in a λ frame, i.e., a frame in which $\lambda = (1, 0)$. Since the parameters of the Lorentz transformation from a general frame to a λ frame can be taken to be⁶ $\beta = \lambda/\lambda_0$ and $\gamma = \lambda_0$, it is clear that the λ -frame momenta become infinite in the infinite λ limit. Therefore Weinberg's analysis⁴ can be carried through

directly in such a frame. This leads back to the results of Sec. II. In particular the new Weinberg variables described by Eqs. (23)–(26) arise in a completely natural way.

It should be noted that Namyslowski²⁹ has also considered variables of this type in his analysis of light front dynamics, and has stressed the fact that they provide a manifestly invariant form for the cluster decomposition property.

As pointed out previously, an important advantage of the variables described by Eqs. (23)–(26) is that their use leads to few-particle equations that are explicitly Lorentz invariant. These variables play a role analogous to the nonrelativistic Jacobi relative momenta, in terms of which nonrelativistic few particle equations are manifestly Galilean invariant. In fact, the relativistic equations developed in Sec. III look very much like their nonrelativistic counterparts. This reflects the existence of a subgroup of the Poincaré group which is isomorphic to the Galilean symmetry group of nonrelativistic quantum mechanics in two dimensions.^{7,8} The variables used here provide a natural way of exploiting this isomorphism.

The similarity between relativistic few-particle equations expressed in terms of the new Weinberg variables and their nonrelativistic counterparts makes the derivation of discontinuity and unitarity relations quite straightforward. The formal procedures are identical to those of nonrelativistic quantum mechanics.^{30,31} The only difference worth noting is the shift in emphasis from the total energy variable to the invariant s variable. It is interesting to note that the method used by Aaron, Amado, and Young²⁴ to derive relativistic three-particle equations from unitarity will lead back to Eq. (54) if the amplitudes are *assumed* to be functions of the variables given by (23)–(25), and the unitarity relation and the production

amplitude are *assumed* to be given by (73)–(75).

It should be noted that it is not quite correct to say that the three-particle equations developed here are *covariant*. The reason is that the equations depend on the *arbitrary* unit vector \hat{u} through its appearance in the η 's and q 's [see Eqs. (23)–(25), (12), and (13)]. It is true, however, that the equations are *invariant* in form, since everything is expressed in terms of the η 's and dot products of the q 's.

Few particle equations obtained from Kadyshevsky's perturbation theory,⁵ as well as the author's CTOPT,⁶ also depend on an external vector, namely, the timelike vector λ which provides an invariant time direction. With these theories it has been shown^{5,6} that if the contributions from the ordered diagrams corresponding to a Feynman diagram are combined, the dependence on λ disappears *on-shell*, and the Feynman result is recovered. This is as it should be, otherwise the S matrix would depend on an arbitrary four-vector, and hence would not be covariant. Since the results obtained here arise from the infinite- λ limit, the dependence on ξ also disappears when the contributions from ordered diagrams are combined and evaluated on shell. It should be noted that it has been proved by Casher³² that the light front scheme is covariant, so this is also as it should be.

Of course the integral equations developed here do not include all of the ordered diagrams corresponding to a Feynman diagram, and moreover are off shell, so the dependence on ξ remains. If the diagrams obtained by reordering the vertices of the diagrams summed by these integral equations are negligible, then the on-shell amplitudes obtained from the solutions of these equations should have negligible ξ dependence. This point is currently under investigation. In this connection it should be noted that Karmanov³³ has investigated the use of an external vector in a relativistic formulation of few particle wave functions and has analyzed to some extent their dependence on the external vector.

As pointed out previously, the diagrams summed in Sec. III to obtain the three-particle equations have a topology similar to the topology of the diagrams that arise in a model for π -N scattering in which it is assumed that the elementary virtual processes are $B \rightleftharpoons B' + \pi$ ($B, B' = N, \Delta, \dots$). Accordingly, it will be possible to use the techniques presented here to develop an invariant, three-dimensional, three-body isobar model for the π -N system, which, moreover, is solvable. It is important to do so, as there is a possibility that some of the low lying resonances seen in π -N elastic scattering are due to the opening of the production threshold, and are not true particle resonances.³⁴ Since it is difficult to explain some of these resonances in terms of quark models,³⁵ this conjecture is certainly worth investigating.

The three-particle equations of Sec. III only take into account $|\psi\rangle$, $|\psi, \phi\rangle$, and $|\psi, 2\phi\rangle$ intermediate states. It is natural to ask if it is possible to do better than this. Recently it was shown³⁶ that *exact* two- and three-particle equations for π -N scattering can be derived from a π -N- Δ field theory with static fermions by using projection operator techniques. If the one-fermion irreducible part of the three-body interaction that appears is neglected, a *closed* set of coupled nonlinear integral equations for all of the quantities of interest is obtained. While these results are very encouraging, the assumption of static fermions raises a question as to their general validity. Since the internal lines in the diagrams considered here are associated with intermediate states, it should be possible to use the projection operator techniques of Ref. 36 to derive exact two- and three-particle equations starting from a covariant field theory. The fact that the topology of LFPT diagrams is similar to those that occur in nonrelativistic theories is further cause for optimism. If it can be shown that the static model results continue to have some validity in the relativistic regime, then it will be possible to investigate three-particle models for the π -N system which go beyond the isobar model.

¹See, for example, J. D. Bjorken and S. Drell, *Relativistic Quantum Mechanics* (McGraw-Hill, New York, 1964); *Relativistic Quantum Fields* (McGraw-Hill, New York, 1964).

²W. Heitler, *The Quantum Theory of Radiation* (Clarendon, Oxford, 1954).

³S. S. Schweber, *An Introduction to Relativistic Quantum Field Theory* (Harper and Row, New York, 1961).

⁴S. Weinberg, *Phys. Rev.* **150**, 1313 (1966).

⁵V. G. Kadyshevsky, *Zh. Eksp. Teor. Fiz.* **46**, 654 (1964) [*Sov. Phys.—JETP* **19**, 443 (1964)]; **46**, 872 (1964) [**19**, 597 (1964)]; *Dok. Akad. Nauk SSSR* **160**, 573 (1965) [*Sov. Phys.—Dokl.* **10**, 46 (1965)].

⁶M. G. Fuda, *Phys. Rev. C* **33**, 996 (1986).

⁷L. Susskind, *Phys. Rev.* **165**, 1535 (1968); in *Lectures in Theoretical Physics*, Vol. XI-D of *Mathematical Methods in Theoretical Physics*, edited by K. T. Mahanthappa and W. E. Britten (Gordon and Breach, New York, 1969).

⁸K. Bardakci and M. B. Halpern, *Phys. Rev.* **176**, 1686 (1968).

⁹S.-J. Chang and S. Ma, *Phys. Rev.* **180**, 1506 (1969).

¹⁰J. Kogut and D. Soper, *Phys. Rev. D* **1**, 2901 (1970); J. D. Bjorken, J. Kogut, and D. Soper, *ibid.* **3**, 1382 (1971).

¹¹R. A. Neville and F. Rohrlich, *Nuovo Cimento* **1A**, 625 (1971); *Phys. Rev. D* **3**, 1692 (1971); F. Rohrlich, *Acta Phys. Austriaca* **8**, 277 (1971).

¹²S.-J. Chang, R. G. Root, and T.-M. Yan, *Phys. Rev. D* **7**, 1133 (1973); S.-J. Chang and T.-M. Yan, *ibid.* **7**, 1145 (1973); T.-M. Yan, *ibid.* **7**, 1760 (1973); **7**, 1780 (1973).

¹³P. A. M. Dirac, *Rev. Mod. Phys.* **21**, 392 (1949).

¹⁴E. E. Salpeter and H. A. Bethe, *Phys. Rev.* **84**, 1232 (1951).

¹⁵D. Lurié, *Particles and Fields* (Interscience, New York, 1968).

¹⁶J. M. Namyslowski, *Phys. Rev. D* **18**, 3676 (1978); P. M. Fishbane and J. M. Namyslowski, *ibid.* **21**, 2406 (1980).

¹⁷J. M. Namyslowski and H. J. Weber, *Z. Phys. A* **295**, 219 (1980).

¹⁸E. H. Wichmann and J. H. Crichton, *Phys. Rev.* **132**, 2788 (1963).

¹⁹G. P. Lepage and S. J. Brodsky, *Phys. Rev. D* **22**, 2157 (1980).

²⁰G. P. Lepage, S. Brodsky, T. Huang, and P. B. McKenzie, in

- Particles and Fields—2*, Proceedings of the Summer Institute, Banff, Alberta, Canada, 1981, edited by A. Z. Capri and A. N. Kamal (Plenum, New York, 1983).
- ²¹S. J. Brodsky and G. P. Lepage, in *Quantum Chromodynamics*, Proceedings of the Summer Institute on Particle Physics, Stanford Linear Accelerator Center, 1979, edited by Anne Mosher, Stanford Linear Accelerator Center, Report SLAC-224, 1980; *Phys. Scr.* **23**, 945 (1981); S. J. Brodsky, T. Huang, and G. P. Lepage, in *Quarks and Nuclear Physics*, Proceedings of the KfK Summer School on Quarks and Nuclear Forces, Bad Liebenzell, Germany, 1981, edited by D. Fries and B. Zeitnitz (Springer, Berlin, 1982).
- ²²S. J. Brodsky, C.-R. Ji, and M. Sawicki, *Phys. Rev. D* **32**, 1530 (1985).
- ²³E. A. Bartnik and J. M. Namyslowski, *Phys. Rev. D* **30**, 1064 (1984).
- ²⁴R. Aaron, R. D. Amado, and J. E. Young, *Phys. Rev.* **174**, 2022 (1968).
- ²⁵J. L. Basevant and R. L. Omnes, *Phys. Rev. Lett.* **17**, 775 (1966).
- ²⁶H. Garcilazo and L. Mathelitsch, *Phys. Rev. C* **28**, 1272 (1983); L. Mathelitsch and H. Garcilazo, *ibid.* **32**, 1635 (1985).
- ²⁷M. G. Fuda, *Phys. Rev. C* **29**, 1222 (1984).
- ²⁸M. G. Fuda, *Phys. Rev. C* **30**, 666 (1984).
- ²⁹J. M. Namyslowski, *Prog. Part. Nucl. Phys.* **14**, 49 (1984).
- ³⁰K. L. Kowalski, *Phys. Rev.* **188**, 2235 (1969); *Phys. Rev. D* **2**, 812 (1970).
- ³¹M. G. Fuda, *Phys. Rev. C* **3**, 485 (1971).
- ³²A. Casher, *Phys. Rev. D* **14**, 452 (1982).
- ³³V. A. Karmanov, *Zh. Eksp. Teor. Fiz.* **71**, 399 (1976) [*Sov. Phys.—JETP* **44**, 210 (1976)]; *Nucl. Phys.* **B166**, 93 (1980); *Zh. Eksp. Teor. Fiz.* **83**, 3 (1982) [*Sov. Phys.—JETP* **56**, 1 (1982)].
- ³⁴B. Blankleider and G. E. Walker, *Phys. Lett.* **152B**, 291 (1985).
- ³⁵L. Tomio and Y. Nogami, *Phys. Rev. D* **31**, 2818 (1985).
- ³⁶M. G. Fuda, *Phys. Rev. C* **31**, 1365 (1985); **32**, 2024 (1985).